FRACTURE ANALYSIS OF CEMENT TREATED DEMOLITION WASTE USING A LATTICE MODEL

DONGXING XUAN, ERIK SCHLANGEN*, ANDRÉ MOLENAAR, LAMBERT HOUBEN

* Faculty of Civil Engineering and Geosciences, Delft University of Technology, Delft 2628 CN, The Netherlands
E-mail: H.E.J.G.Schlangen@tudelft.nl

Key words: Cement treated demolition waste, Lattice model, Fracture, Indirect tensile strength

Abstract: Fracture properties of cement treated demolition waste were investigated using a lattice model. In practice the investigated material is applied as a cement treated road base/subbase course. The granular aggregates used in this material were crushed recycled concrete and masonry. This results in six different types of phases in the mixture: recycled concrete, recycled masonry, mortar, interface between recycled concrete and mortar, interface between recycled masonry and mortar and interface between recycled concrete and masonry.

In order to numerically analyze the fracture behavior of cement treated demolition waste, a cross section image of a cylindrical specimen (Φ150mm) for monotonic indirect tensile test (ITT) was digitized and processed to obtain a multiphase lattice image showing every individual phase. The mesh area used for the lattice model was 1 mm^2. Simulation results show that when the simulated ITT loading direction varies on the image, the simulated indirect tensile strengths (ITS) have a larger scatter compared to the variation of experimental results of ITS in the laboratory. This indicates that the numerical simulation of cemented granular demolition waste using a 2D lattice model is strongly influenced by the loading direction on the simulated image. This should be because of high heterogeneity of the mixture, especially the arrangement of aggregates along the loading direction. With a model correlation factor 2, the average simulated ITS that is obtained under different loading directions on one image is comparable to the experimental ITS.

1 INTRODUCTION

Cement treated granular materials (CTG$_r$Ms) consist of a densely packed particle skeleton and cement mortar filling in the pore and bonding to the coarse particles. In the field of road pavement, CTG$_r$Ms are particularly used to enhance the bearing capacity of the pavement structure. Therefore, they have been widely applied as road base and/or sub-base in many countries [1].

In general CTG$_r$Ms as road base materials are produced by using high quality coarse natural or crushed aggregates. Because of shortage of natural aggregates and environmental impact of construction and demolition waste (CDW), CDW is recycled in a number of countries and now promoted as a sustainable road base/sub-base material. The authors have done a series of researches into the material properties of cement treated recycled demolition waste with crushed recycled concrete and masonry (CTM$_i$G$_r$). The investigated mechanical properties include strength (f), elastic modulus (E) and drying shrinkage behaviour [2-5]. Estimation models for the mechanical properties and shrinkage behaviour have been developed in relation to mixture variables like cement content (C), water content (W), dry density (D), masonry content (M) and curing time (t).

Traditionally, the failure of CTG$_r$Ms originates either in a discontinuity in the internal structure (the matrix) or in the bonding layer between aggregates and matrix

[6]. When recycled CDW aggregates are used, the failure of CTM_iG_r becomes complicated due to the existence of more components, especially the lower strength of the recycled masonry aggregates (RMA) and their interfaces. Therefore, failure can also occur within the RMA.

In fact the quality of the masonry rubble collected for producing the RMA can vary considerably[7]. The variation of the mechanical properties of RMA produced by using recycled masonry rubble can influence the failure behaviour of CTM_iG_r. In practice that would mean that extensive testing is needed in order to explore the influence of the RMA variation and its mechanical properties on the failure of CTM_iG_r. There is however also another way to explore this by means of numerical simulation.

So far three main approaches exist for modelling fracture and cracking in engineering materials (concrete, rock, masonry, et al.), namely discrete crack modelling, smeared crack modelling and lattice modelling [8, 9]. In the 1970s the smeared crack modelling gained much popularity because of the preservation of the original finite element mesh. Recently, lattice models have become popular for explaining fracture processes at a detailed level. In the sequel of this paper the lattice model is chosen to analyze the fracture process of CTM_iG_r.

2 INVESTIGATED MATERIAL

Two types of main recycled materials in CDW, recycled crushed concrete (RCA) and recycled crushed masonry (RMA), were used to prepare the cement treated demolition waste as shown in Figure 1. The mixture was composed of 65% RMA by mass, 35% RCA by mass, 4% cement (Portland cement CEM I 42.5) by mass of the total aggregates and 10.94% water by mass of the total aggregates.
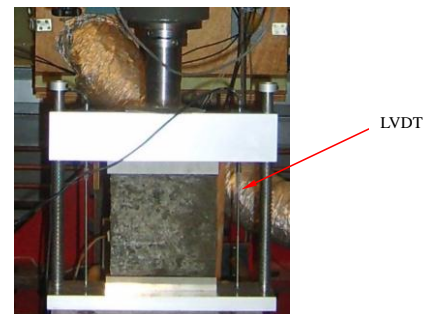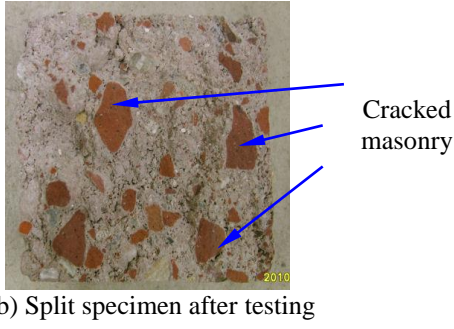

(a) RMA

(b) RCA

Figure 1: Crushed masonry (a) and concrete (b) aggregates (with a size of 22.4-31.5 mm).

The monotonic indirect tensile test (ITT) of CTM_iG_r with a size of $\Phi150\times150$ mm was performed by using the set-up in Figure 2. It was done by using a 150 kN MTS actuator in the displacement controlled mode. The displacement rate chosen for the ITS was 0.2 mm/second and was controlled by two LVDTs. The data of the force and the vertical deformation were automatically recorded. Note that the weak masonry particles can be broken and cracks go through them as shown in Figure 2.
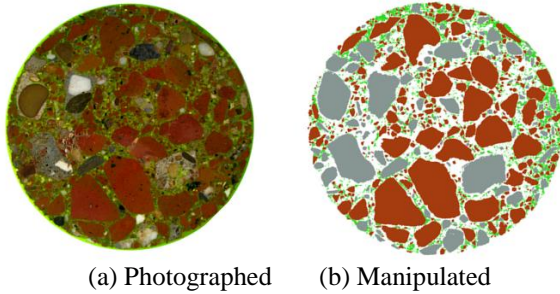

LVDT

(a) Set-up for indirect tensile test

(b) Split specimen after testing

Figure 2: Set-up for indirect tensile test (a) and split specimen after testing (b).

3 CONSTRUCTION OF LATTICE MODEL

3.1 Implementation of heterogeneity

Before constructing the lattice image for a real mixture, several steps were performed. Firstly, a diametrical cross section of a cylindrical specimen with a diameter of 150 was impregnated with a resin and a slice was cut from the sample and photographed by means of a digital camera with a high resolution (see Figure 3(a)). On basis of the color or gray differences, this image was manipulated by Adobe Photoshop CS4 to distinguish different aggregates (RCA and RMA), mortar and voids as shown in Figure 3(b).
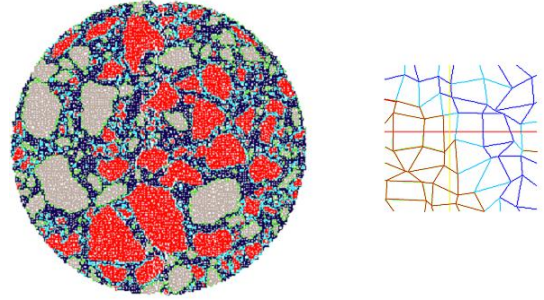

(a) Photographed   (b) Manipulated

Figure 3: Image of a diametrical cross section of CTM_iG_r used in the monotonic ITT (red: RMA; gray: RCA; white: matrix or mortar; green: void filled by resin).

In this research the lattice analysis was conducted on this image with a diameter of 150 mm and with a thickness of 1 mm. The shape of the lattice beam was cylindrical. The mean length of the beam was equal to 1 mm. The radius of the beam was then calculated by:

$$\pi \cdot r^2 = 1 = 1 \ mesh \ area \qquad (1)$$

By using the GLAK software developed at TU Delft [10], the random quadrangular mesh lattices were tagged on the specimen as shown in Figure 4. Note that depending on the position of the phases in the mixture, each type of beam element is colorized. In fact there are six types of beam elements: the RMA, the RCA, the mortar with voids, the interface between RMA and mortar, the interface between RCA and mortar and the interface between RMA and RCA. The last one is bound by a thin layer of cement paste with fine aggregates, which is assumed to have similar properties as the mortar. Therefore, only five phases were evaluated.

Figure 4: Random quadrangular mesh lattices for a real mixture (red: RMA; gray: RCA; dark blue: mortar; light blue: interface between RMA and mortar; green: interface between RCA and mortar)

3.2 Fracture criterion

In the lattice model all the beam elements have fixed connections in the nodes. Therefore, every beam can transfer a normal force, a shear force and a bending moment. Each beam is herein supposed to behave linear elastic and brittle under tensile stress. Fracture is mimicked by sequential removal of beam elements where the stress exceeds the tensile strength. The tensile stress of the beam elements can be derived from the Formula:

$$\sigma_t = \frac{N}{A} + \alpha \cdot \frac{(|M_i|, |M_j|)_{max}}{W} \qquad (2)$$

Where, N stands for the normal force; A represents the area of the cross section; α is a bending factor; $|M_i|, |M_j|$ refer to the bending moments at both ends of a beam; W is a

3

geometric parameter.

4 FAILURE CHARACTERISTICS

4.1 Mechanical properties of each phase

In order to be able to establish the relationship between composition and property of CTM_iG_r in a numerical way, it is first of all necessary to characterize the mechanical properties of every phase in CTM_iG_r and use these as input values for the numerical analysis. As shown in Figure 4, there are six phases in the mixture of CTM_iG_r: the RMA, the RCA, the mortar composed of fine aggregates (less than 2 mm) and cement paste, the interface between RMA and mortar, the interface between RCA and mortar and the interface between RMA and RCA. The properties of these five phases were determined for a mixture with 65% RMA by mass, 4% cement by mass and 101% degree of compaction, which was cured for 28 days.

Figure 5 shows the meso-scale compression-tension test setup. The tested sample shown was the recycled masonry with a size of Φ 9×18 mm. By using this setup, the direct tensile strength of the five phases from the mixture was measured.
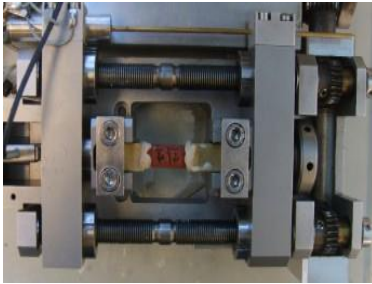

Figure 5: Meso-scale compression-tension test setup.

Table 1 lists the measured direct tensile strength (f_t) of the above five phases and the estimated mechanical properties. Some empirical models used to estimate other mechanical properties, such as compressive strength (f_c), elastic modulus (E) and shear modulus (G), are obtained from previous references [11-13].

Table 1: Mechanical properties of six phases in CTM_iG_r at 28 days (with 65% RMA by mass, 4 % cement by mass, 101% degree of compaction and 10.94% water).

Phases	f_t (MPa)	f_c (MPa)	E (MPa)	G (MPa)
Mortar	0.79	-7.9	1780	770
Interface between mortar and RMA	0.23	-2.3	520	210
Interface between Mortar and RCA	0.61	-6.1	1380	570
RMA	1.81	-17.1	6820	2840
RCA	2.72	-27.2	29130	12140
Interface between RMA and RCA	0.79	-7.9	1780	770

4.2 Fracture simulation of the mixture

In this research the loading locations on the image were modelled on four nodes connected with beam elements on the top and bottom as shown in Figure 6. Meanwhile, these connected elements are set as unbroken elements. Note that the modelling was such that there was no relative displacement between the specimen and the simulated loading nodes. With increasing the vertical deformation, some lattice elements will fail at different levels of loading force. The change of the loading force was then used to describe the crack opening related to the fracture process.
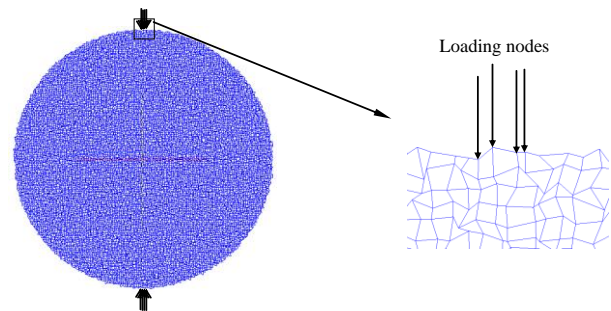

Figure 6 Illustration of simulation loading on the specimen.

The results of the numerical analysis of the fracture process are illustrated in Figure 7. The simulated load-vertical displacement curve is plotted in Figure 8. During the fracture process, a vertical or splitting macro-crack develops between 900 and 1200 simulation steps. This crack causes the first load peak in Figure 8.

Moreover, this crack does cross the

4

specimen along its complete height, but stops next to the loading elements. This is because of the high compressive vertical and horizontal stresses in that area. When continuing the simulation, the second load peak in Figure 8 occurs. This peak is related to the initiation and propagation of radial cracks from the adjacent loading elements and the edge of the specimen inwards.
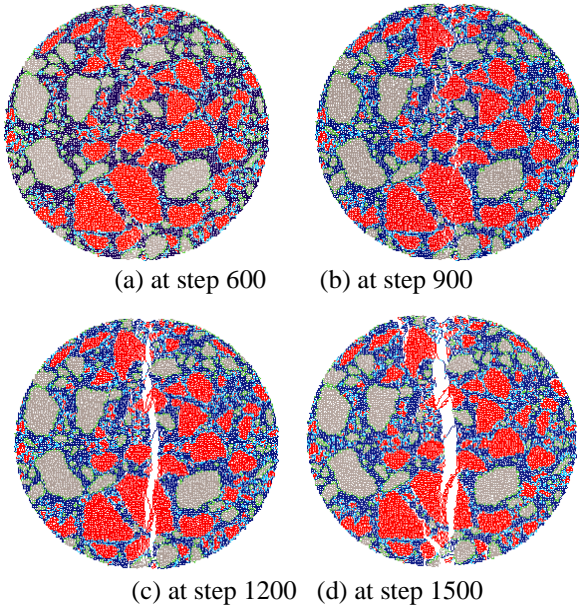

(a) at step 600   (b) at step 900

(c) at step 1200   (d) at step 1500

Figure 7: Lattice analysis of a monotonic ITS testing (The displacements are scaled by factor 20).
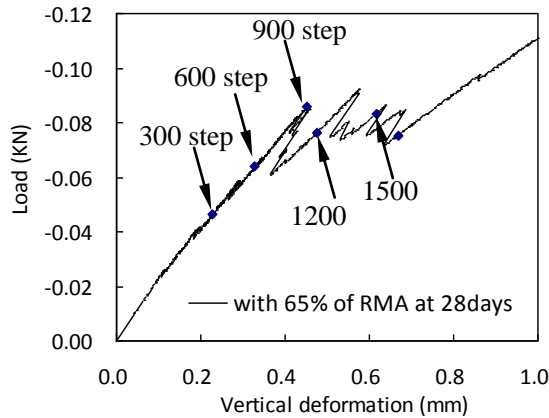

Figure 8: Simulated load-vertical displacement diagram.

In the real ITT, the loading platens were not fixed or glued onto the specimen. This is different from the simulation in which it was assumed that there was no relative displacement between the specimen and the simulated loading platens. When the main splitting crack propagates through the specimen, the specimen will split in two halves and the loading platens get disconnected with the specimen. This means that the first load peak shows the strength of the specimen. According to the experimental results, no radial cracks were observed in the specimen and only the primary crack goes through the specimen as shown in Figure 2. This further supports the conclusion that the first simulated load peak is related to the strength of the specimen.

As the aim of this numerical work was mainly to evaluate the influence of RMA and its ITS on the fracture behaviour, no special effort was put into perfectly to reproduce the experimentally observed stress-strain characteristics in the simulation. The simulated load-displacement diagram used for analysis in this study is the segment until the main vertical splitting crack has completely developed.

4.3 Simulated ITS of the mixture

Note that the implementation of the lattice simulation is on a cross-section image of one specimen along one direction. In fact, the loading direction on this image can also be random. In order to explore the influence of the loading orientation on the simulation result, several simulations were carried out considering different loading orientations on the prepared image (negative means anti-clockwise), as shown in Figure 9.
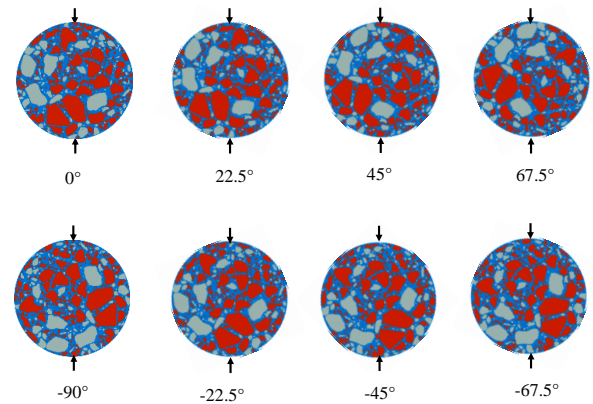

Figure 9: Different loading orientations on the image.

Table 2 shows the influence of the loading orientation on the simulated ITS and vertical deformation. It can be seen that the loading direction on the simulated image determines the variation of the simulated ITS. The simulated ITS can range from 0.26 MPa to 0.44 MPa. The coefficient of variation of the vertical deformation at failure and the simulated ITS is high, 27% and 16%, respectively.

Table 2: Variation of simulated results.

Loading orientation	Simulated deformation at peak (mm)	Simulated force at peak (kN)	Simulated ITS (MPa)
0°	0.46	0.085	0.36
22.5°	0.35	0.071	0.30
45.0°	0.52	0.083	0.35
67.5	0.19	0.097	0.41
-22.5°	0.36	0.061	0.26
-45.0°	0.25	0.104	0.44
-67.5°	0.39	0.102	0.43
-90.0°	0.40	0.094	0.40
Mean	0.37	0.087	0.37
Standard deviation	0.10	0.014	0.06
Coefficient of variation	27%	16%	16%

4.4 Comparison with measured ITS of the mixture

In order to be able to compare the simulation results to the experiment results, five CTM_iG_r specimens were tested and their results are shown in Table 3.
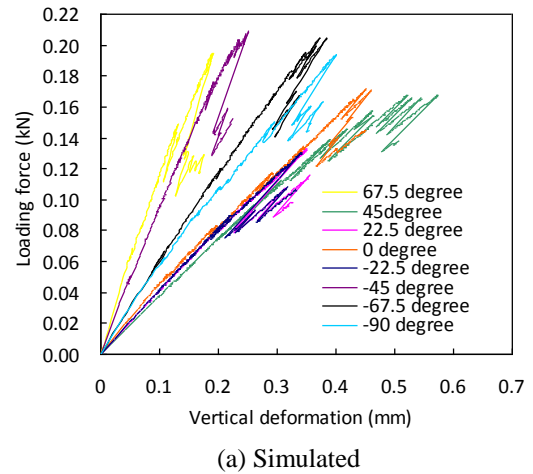
Table 3: Variation of experimental results.

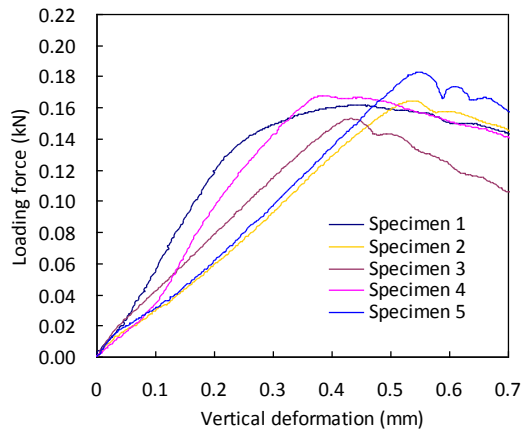| Items	Vertical deformation at peak (mm)	Failure force at peak (kN)	Experimental ITS (MPa)
1	0.44	0.176	0.75
2	0.54	0.174	0.74
3	0.43	0.168	0.67
4	0.39	0.172	0.73
5	0.55	0.188	0.80
Mean	0.47	0.174	0.74
Standard deviation	0.07	0.009	0.04
Coefficient of variation	15%	5%	5%

Note that the experimental ITS can range from 0.67 MPa to 0.80 MPa. Its coefficient of variation is much lower than that of the simulated results. This could be because the experimental test is performed on a 150 mm-thickness specimen, while the simulation is only done on a 2D level. And so the influence of specimen heterogeneity along the loading direction on a 150 mm thick specimen is limited and its variation becomes lower.

Meantime, it is noticed that the simulated force in Table 2 should be multiplied with a factor of 2.0 in order to obtain an ITS value which is comparable to the experimental one. This parameter should be a constant lattice model parameter for this simulated monotonic ITT. It could be sourced from the geometry definition and configuration of the lattice model.

$$Factor = \frac{Experimental\ ITS}{Simulated\ ITS} = \frac{0.74}{0.37} = 2.0 \quad (3)$$

Figure 10 further shows all simulated load-vertical displacement diagrams compared to the measured ones. Figure 10(a) includes the above-mentioned factor 2.0. Although the simulated curves show rather brittle behavior compared to the experimental curves, they are comparable to the experimental ITS results.

(a) Simulated

(b) Experimental

Figure 10: Simulated and experimental load-displacement curves.

5 CONCLUSIONS AND RECOMMENDATIONS

In this paper the lattice model was used to simulate the monotonic ITS of cement treated demolition waste. Some main findings of the numerical analyses are given below.

1) The loading direction on the 2D mixture image influences the simulated ITS. Moreover, this can result in a bigger variation of the simulated ITS compared to the experimental results. This should be because of the influence of high heterogeneity of the specimen along the loading direction.

2) The simulated force of the monotonic ITT lattice model at failure needs to be corrected with a factor of 2 in order to get comparable results obtained experimentally. This factor is a lattice model parameter for the monotonic ITT.

3) The average result of the corrected simulated ITS from several lattice simulations with different loading orientations can represent the average experimental ITS of the CTM_iG_r mixture.

4) The ITT lattice model is capable to simulate the fracture process of CTM_iG_r. It can describe the load-displacement curve until failure occurs across the specimen diameter.

It is recommended that more effort should be made to improve the construction of the lattice model, such as the change of the geometrical definition of the beam lattice, the connection between the loading plates and the specimen and a combined failure criterion of compression and tension. The purpose is to reproduce the experimentally observed stress-strain characteristics of CTM_iG_r more precisely.

REFERENCES

[1] Terrel, R. L., Epps, J. A., Barenberg, E. J., Mitchell, J. K., and Thompson, M. R., 1979 (b). *Soil Stabilization in Pavement Structures, a User's Manual-Volume 2: Mixture Design Considerations (No. FHWA-IP-80-2).* Washington D.C: Federal Highway Administration, Department of Transportation.

[2] Xuan, D. X., Houben, L. J. M., Molenaar, A. A. A., and Shui, Z. H. Prediction of the Mechanical Properties of Cement Treated Mix Granulates. *The TRB 90th Annual Meeting on CD, 2011,Washington, D.C.*

[3] Xuan D.X., Molenaar A.A.A., and Houben L.J.M., 2012. Compressive and Indirect Tensile Strengths of Cement Treated Mix Granulates with Recycled Masonry and Concrete Aggregates. *Journal of Materials in Civil Engineering, 24(5):*577-585.

[4] Xuan, D. X., Houben, L. J. M., Molenaar, A. A. A., and Shui, Z. H., 2012. Mixture Optimization of Cement Treated Demolition Waste with Recycled Masonry and Concrete. *Materials and Structures,* 45(12): 143-151.

[5] Xuan, D. X., Houben, L. J. M., and Molenaar, A. A. A. Deformation Behavior of Cement Treated Recycled Mix Granulates. *The TRB 91st Annual Meeting on CD, 2012,Washington, D.C.*

[6] Williams, R. I. T., 1986. *Cement-treated Pavements: Materials, Design, and Construction.* London: Elsevier Applied Science Publishers.

[7] Hansen, T. C., 1992. *Recycling of Demolished Concrete and Masonry:*

Report of Technical Committee 37-DRC, Demolition and Reuse of Concrete. (1st ed.). London; New York: E & FN Spon.

[8] Galvez, J. C., Cervenka, J., Cendon, D. A. and Saouma, V., 2002. A Discrete Crack Approach to Normal/Shear Cracking of Concrete. *Cement and Concrete Research*, 32(10):1567-1585.

[9] Schlangen, E. and Garboczi, E. J., 1997. Fracture Simulations of Concrete Using Lattice Models: Computational Aspects. *Engineering Fracture Mechanics*, 57(2-3): 319-332.

[10] Qian, Z., Schlangen, E., Ye, G. and van Breugel, K., 2011. 3D Lattice Fracture Model: Theory and Computer Implementation. *Key Engineering Materials,* 452-453: 69-72.

[11] EN199-1-1, 2005. *Design of Concrete Structures-Part 1-1: General Rules and Rules for Buildings.* Brussels: Europe Committee for Standardization.

[12] Larrard, F. d., 1999. *Concrete Mixture Proportioning: a Scientific Approach.* London ; New York: E & FN Spon.

[13] Vermeltfoort, A. T., 1997. Properties of Some Clay Bricks Under Varying Loading Conditions. *Masonry Intern*